

# 一步电沉积法制备 Ni-Mo-Nd/NF 复合电极 及其析氢性能研究

尹志芳<sup>1</sup>, 刘卫<sup>1,2\*</sup>, 杨泱<sup>2</sup>, 陈星<sup>2</sup>, 廖惠怡<sup>1</sup>

(1.湖南城市学院 材料与化学工程学院, 湖南 益阳 413000;  
2.益阳鸿源稀土有限责任公司, 湖南 益阳 413001)

**摘要:** 目的 采用一步恒电流沉积法在泡沫镍基底上制备出镍-钼-钕三元析氢电极, 提高碱性条件下的析氢性能。方法 使用电化学工作站研究工艺参数对 Ni-Mo-Nd/NF 析氢电极性能的影响, 同时制备 Ni-Mo/NF 析氢电极, 使用扫描电镜 (SEM)、X 射线衍射分析仪 (XRD)、能谱仪 (EDS) 和 X 射线光电子能谱 (XPS) 对合金镀层表面形貌、相结构、元素含量及成键状态进行表征。通过线性扫描伏安法 (LSV)、循环伏安法 (CV) 及电化学阻抗技术 (EIS) 测试电极析氢性能。结果 最佳工艺参数为: pH=4.5, 电流密度 30 mA/cm<sup>2</sup>, 沉积时间 60 min, 温度 30 °C。在 1.0 mol/L KOH 溶液中, Ni-Mo-Nd/NF 电极在 10 mA/cm<sup>2</sup> 下的析氢过电位仅为 73 mV, Tafel 斜率为 147 mV/dec, 表明析氢反应机理遵循典型的 Volmer-Heyrovsky 步骤。此外, Ni-Mo-Nd/NF 电极在长时电解 24 h 时电流密度保持稳定, 2 000 次循环伏安测试后, 催化剂的活性衰减微小。结论 稀土元素 Nd 的掺杂, 能够细化电极表面的球形颗粒并提高电极表面粗糙度, 从而提升电极的比表面积, 为析氢反应提供更多的活性位点, 利于析氢反应效率的提高。由于三元合金的协同作用, 与二元合金 Ni-Mo/NF 相比, Ni-Mo-Nd/NF 三元合金电极显示出更优异的 HER 催化性能。

**关键词:** 一步电沉积; Ni-Mo-Nd/NF; 析氢反应; 泡沫镍

**中图分类号:** TG174    **文献标志码:** A    **文章编号:** 1001-3660(2024)06-0214-08

**DOI:** 10.16490/j.cnki.issn.1001-3660.2024.06.020

## One-step Electrodeposition of Ni-Mo-Nd/NF Electrodes and Their Hydrogen Evolution Performance

YIN Zhifang<sup>1</sup>, LIU Wei<sup>1,2\*</sup>, YANG Yang<sup>2</sup>, CHEN Xing<sup>2</sup>, LIAO Huiyi<sup>1</sup>

(1. College of Materials and Chemical Engineering, Hunan City University, Hunan Yiyang 413000, China;  
2. Yiyang Hongyuan Rare Earth Co., Ltd., Hunan Yiyang 413001, China)

**ABSTRACT:** Finding non-precious metal hydrogen evolution reaction (HER) electrocatalysts with high efficiency and low cost is a great challenge. One-step galvanostatic deposition method was used to prepare nickel-molybdenum-neodymium ternary hydrogen evolution electrode on nickel foam substrate and improve its hydrogen evolution performance under alkaline condition. The effects of process parameters on the performance of Ni-Mo-Nd/NF hydrogen evolution electrode were studied by

收稿日期: 2023-02-10; 修订日期: 2023-07-08

Received: 2023-02-10; Revised: 2023-07-08

基金项目: 益阳市银城科技人才托举工程项目 (益人才办 (2022) 6 号)

Fund: Yiyang Yincheng Science and Technology Talent Supporting Project (Yi Talent Office (2022) No. 6)

引文格式: 尹志芳, 刘卫, 杨泱, 等. 一步电沉积法制备 Ni-Mo-Nd/NF 复合电极及其析氢性能研究[J]. 表面技术, 2024, 53(6): 214-221.  
YIN Zhifang, LIU Wei, YANG Yang, et al. One-step Electrodeposition of Ni-Mo-Nd/NF Electrodes and Their Hydrogen Evolution Performance[J]. Surface Technology, 2024, 53(6): 214-221.

\*通信作者 (Corresponding author)

electrochemical workstation, and the Ni-Mo/NF hydrogen evolution electrode was prepared simultaneously. Scanning electron microscopy (SEM), X-ray diffraction (XRD), energy dispersive spectroscopy (EDS) and X-ray photoelectron spectroscopy (XPS) were used to characterize the surface morphology, phase structure, element content and bonding state of the alloy coating. The hydrogen evolution performance was measured by linear sweep voltammetry (LSV), Cyclic voltammetry (CV) and electrochemical impedance spectroscopy (EIS). Throughout the electrodeposition experiment, the NF (10 mm×10 mm×0.3 mm), the graphite plate (20 mm×20 mm×5 mm) and the saturated calomel electrode (SCE) were used as working, counter, and reference electrodes, respectively. The results showed that the optimum process parameters were pH=4.5, current density 30 mA/cm<sup>2</sup>, deposition time 60 min and temperature 30 °C. After electrochemical deposition, the surface of Ni-Mo/NF alloy coating presented cellular structure with relatively coarse particles. With the introduction of Nd element, the surface particles of Ni-Mo-Nd/NF coating increased, and the fine particles grew directly on the conductive substrate, which increased the specific surface area of the coating, provided more the active sites of hydrogen evolution, and helped to improve hydrogen evolution efficiency. According to Mapping, Ni, Mo and Nd were evenly distributed on the coating, and their mass percentages were 57.0%, 29.9% and 13.1% respectively. It could be seen from XRD that with the doping of Mo and Nd, the peak appeared negative shift, which might be due to the solid solution of Mo and Nd in Ni, and the Ni atom was replaced by the Nd atom with a larger radius, and the lattice changed. Ni 2p, Mo 3d and Nd 3d peaks could be clearly observed in the XPS total spectrum. In terms of electrochemical performance, the over potential of Ni-Mo-Nd/NF was only 73 mV at 10 mA/cm<sup>2</sup> in alkaline medium, the Tafel slope was 147 mV/dec, the double-layer capacitance ( $C_{dl}$ ) value was 4.39 mF/cm<sup>2</sup>, the charge transfer resistance was 1.352 Ω, compared with Ni-Mo/NF. The binary electrode decreased by 62 mV, 54 mV/dec, 0.35 Ω, and the double-layer capacitance ( $C_{dl}$ ) value increased by 1.66 mF/cm<sup>2</sup>. In addition, the current density of Ni-Mo-Nd/NF electrocatalyst remained stable after prolonged electrolysis for 24 h, and the activity of the catalyst decreased slightly after 2 000 cycles of voltammetry. It is concluded that the doping of rare earth element Nd can increase and refine the crystal grains, thus increasing the specific surface area of the electrode, providing more active sites for hydrogen evolution reaction and improving the efficiency of hydrogen evolution reaction. Compared with the binary alloy Ni-Mo/NF, the Ni-Mo-Nd/NF ternary alloy electrode exhibits better HER catalytic performance due to the synergistic effect of the ternary alloy.

**KEY WORDS:** one-step electrodeposition; Ni-Mo-Nd/NF; hydrogen evolution reaction; nickel foam

氢 (H<sub>2</sub>) 作为一种清洁高效的二次能源, 由于其高能量密度 (143 MJ/kg) 和零排放<sup>[1]</sup>的特性, 是较有前途的替代能源之一。在众多制氢技术中, 电催化裂解水制氢反应 (HER) 作为一种具有代表性的能量转换技术而备受关注。贵金属如 Pt、Pd、Rh 等作为析氢催化电极, 析氢过电位较低, 但由于其稀缺性和成本较高, 难以在工业实践中广泛应用<sup>[2-4]</sup>。因此, 寻找性价比高和析氢活性高的电极材料具有重要的现实意义。在过渡金属析氢合金中, 因形成高粗糙度的电极表面及多孔结构的电极微观形貌, Ni-Mo 合金被证明是在碱性溶液中析氢性能较好二元析氢材料之一<sup>[5-7]</sup>。Liu 等<sup>[8]</sup>研究了四元 Ni-Ce-Pr-Ho 合金的析氢性能, 结果表明, 以泡沫镍 (Nickel Foam, NF) 为基体, 加入稀土元素后合金的析氢催化活性及电导率明显提高, 同时在碱性环境中的耐腐蚀性也明显增强。Zhu 等<sup>[9]</sup>研究的 Ni-Co-B-RE (RE=Ce, Gd, Nd) 材料的  $\eta_{10}=92$  mV, 具有优良的 HER 活性。Nd 的加入细化了包膜晶粒的表观形貌, 有效地提高了电极活性。

本文将稀土 Nd 掺杂到 Ni-Mo 电催化剂中, 采用恒流电沉积法制备了一种新型的 Ni-Mo-Nd 电催化剂。研究了 Ni-Mo-Nd/NF 电极在 1.0 mol/L KOH 溶液

中的电化学行为以及在电流密度为 10 mA/cm<sup>2</sup> 时, Ni-Mo-Nd/NF 的析氢电极过电位。

## 1 试验

### 1.1 电极的制备

在整个电沉积实验中, 以 NF (10 mm×10 mm×0.3 mm) 为工作电极, 石墨板 (20 mm×20 mm×5 mm) 为对电极, 以饱和甘汞电极 (SCE) 为参比电极。在电沉积之前, 先对 10 mm×20 mm NF 进行预处理, 分别用 10% (质量分数) 盐酸、无水乙醇依次超声清洗活化 15 min, 再用去离子水冲洗 3 次, 在 60 °C 真空干燥箱干燥 8 h。样品沉积后, 用去离子水和无水乙醇交替清洗, 然后在室温下风干。

采用单因素实验法探究各因素对镀层析氢催化性能的影响, 得到 Ni-Mo-Nd/NF 复合电极的最佳制备工艺, 最佳沉积参数为 pH 值 4.5, 电流密度 30 mA·cm<sup>-2</sup>, 沉积时间 60 min 及温度 30 °C, 电解质组成见表 1, 在此基础上, 制备了 Ni-Mo 电极与之对比。同时制备了 Pt/C 电极, 制备方法为: 称取 10 mg 含 Pt 量 20% (质量分数) 的 Pt/C 粉末, 将其均匀分

表 1 Ni-Mo/NF 和 Ni-Mo-Nd/NF 电催化剂电沉积的电解质组成

Tab.1 Electrolyte composition of Ni-Mo/NF and Ni-Mo-Nd/NF electrocatalysts during electrodeposition

| Electrolyte composition  | Ni-Mo/(g·L <sup>-1</sup> ) | Ni-Mo-Nd/(g·L <sup>-1</sup> ) |
|--|----------------------------|-------------------------------|
| NiSO <sub>4</sub> ·6H <sub>2</sub> O   | 33.33                      | 33.33                         |
| (NH <sub>4</sub> ) <sub>6</sub> Mo <sub>7</sub> O <sub>24</sub> ·4H <sub>2</sub> O | 20                         | 20                            |
| NdCl <sub>3</sub>  | —                          | 2                             |
| C <sub>7</sub> H <sub>6</sub> O <sub>6</sub> S·2H <sub>2</sub> O                   | 13.33                      | 13.33                         |
| C <sub>6</sub> H <sub>5</sub> Na <sub>3</sub> O <sub>7</sub> ·2H <sub>2</sub> O    | 20                         | 20                            |
| H(OCH <sub>2</sub> CH <sub>2</sub> ) <sub>n</sub> OH                               | 6.66                       | 6.66                          |
| NaCl   | 20                         | 20                            |
| H <sub>3</sub> BO <sub>3</sub>   | 13.33                      | 13.33                         |

散到 440 μL 混合溶液中 (400 μL 无水乙醇和 40 μL 质量分数为 0.5% Nafion)，超声 30 min 后取 10 μL 混合液滴涂在玻碳电极 ( $d=3$  mm) 表面，室温干燥，得到负载量为 3.21 mg/cm<sup>2</sup> Pt/C 电极。

## 1.2 样品表征及电化学性能测试

样品采用 X 射线衍射仪 (XRD, 荷兰帕纳科公司), 扫描电子显微镜 (SEM, 捷克泰思肯), X 射线能谱 (EDS, 美国 KRATOS 公司), X 射线光电子能谱 (XPS, 美国赛默飞公司) 对电极材料的表面形貌、相结构、元素含量及成键状态进行表征。采用电化学工作站 (上海辰华 660E) 进行相关电化学性能测试。在三电极测试体系中, 电沉积制备的镀层电极为工作电极, 石墨电极为对电极, 饱和甘汞电极作为参比电极, 1.0 mol/L KOH 溶液为电解液。为了直接比较标准化电位, 根据下面的 Nernst 方程<sup>[10]</sup>, 将测试所得电位值 (vs. SCE) 换算为相对标准氢电位 (vs. RHE):  $E_{\text{RHE}} = E_{\text{SCE}} + 0.242 + 0.059 \times \text{pH} - 0.000791 \times (T - 298.15) - iR$ 。线性扫描伏安曲线 (LSV) 扫描速度为 2 mV/s, 根据 Tafel 方程<sup>[11]</sup>:  $\mu = a + b \lg J$  计算 Tafel 斜率, 其中  $\mu$ 、 $b$ 、 $J$  分别表示过电位、Tafel 斜率和电流密度; 电化学阻抗谱 (EIS) 测试频率为  $10^5$ ~ $10^{-2}$  Hz, 过电位为 200 mV, 采用 Z-view 软件 (Scribner Associates, Inc.) 对 EIS 数据进行拟合计算; 循环伏安曲线 (CV) 在 0.1 V/s 扫描速度下测定样品, 在 10~100 mV/s 的扫描速率下, 在非法拉第区间测量曲线, 计算电化学活性表面积 (ECSA); 循环伏安曲线 (CV) 在不同扫描速率 (10~100 mV/s) 下研究了电催化剂非法拉第区间电化学双层电容 ( $C_{dl}$ ), 所有电化学测试都在恒温 25 °C 下进行。

## 2 结果与讨论

### 2.1 表面形貌分析

图 1a~b、图 1c~d 分别为 Ni-Mo/NF、Ni-Mo-Nd/NF 电极的扫描电子显微镜 (SEM) 照片。电化学沉积之

后, Ni-Mo/NF 二元合金镀层的表面呈胞状结构, 颗粒相对粗大; 随着 Nd 元素的引入, Ni-Mo-Nd/NF 镀层表面颗粒增加, 细小颗粒直接生长在导电衬底上, 这提升了镀层比表面积, 增加了析氢的活性位点, 有利于析氢<sup>[12-13]</sup>。同时根据图 2 可知, Ni、Mo 及 Nd 3 种元素在镀层上均匀分布, 其质量分数分别为 57.0%、29.9% 和 13.1%。

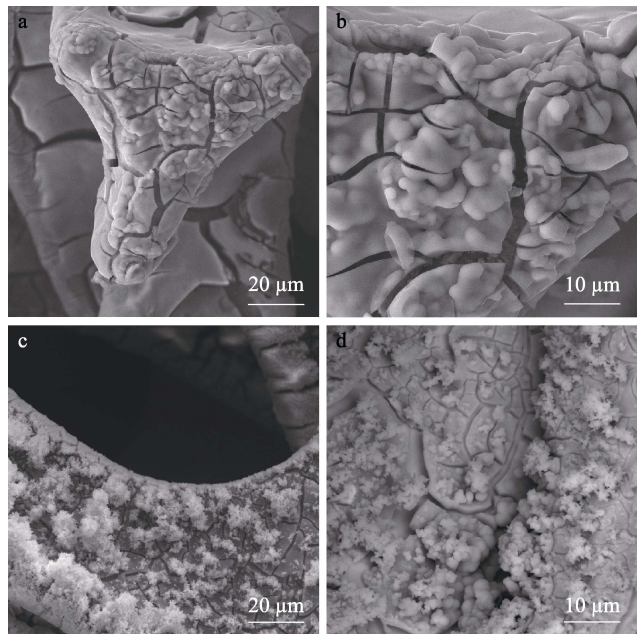


图 1 Ni-Mo/NF 的 SEM 图(a~b);  
Ni-Mo-Nd/NF 的 SEM 图(c~d)  
Fig.1 SEM images of Ni-Mo/NF (a-b) and  
SEM images of Ni-Mo-Nd/NF (c-d)

为进一步揭示 Ni-Mo-Nd/NF 电极的晶体结构, 首先将电极上刮下来的样品粉末进行 XRD 测试, 图 3 为 Ni-Mo-Nd/NF 电极与纯 Ni 的 XRD 对比图。从图 3 可以看到 3 个峰值, 在  $2\theta$  约为 44.4°、51.7° 和 76.2° 时出现衍射峰, 分别对应于 Ni 的 (111)、(200) 和 (220) 晶面的 3 个标准衍射峰。结果表明, 制备的 Ni-Mo-Nd/NF 电极与 NF 电极有极其相似的晶体结构, 归因于 Mo 与 Nd 在 Ni 基体中的高溶解度。Mo 和 Nd 元素引入后, XRD 谱图中没有发现主衍射峰, 说明 Mo 和 Nd 取代 Ni 原子形成富 Ni 结构<sup>[14-15]</sup>。如图 3b~d 所示, Mo 和 Nd 掺杂后峰出现负偏移, 这可能是由于 Mo 和 Nd 在 Ni 中固溶, Ni 原子被半径较大的 Nd 原子取代, 晶格发生了变化<sup>[16-17]</sup>。

利用 XPS 对 Ni-Mo-Nd/NF 电催化剂表面的元素组成和成键状态进行分析, 如图 4 所示。将 XPS 数据与标准的 XPS 手册进行比较, 在 XPS 总光谱中可清晰观察到 Ni 2p、Mo 3d、Nd 3d、C 1s 及 O 1s 峰。

O 1s 峰在 531.6 eV 左右, 这可能是由于催化剂表面吸附了少量的含氧基团所致<sup>[18]</sup>。在 284.8 eV 处检测到的 C 1s 峰是由测试仪器中的碳信号所致<sup>[19]</sup>。Ni 2p 的光谱如图 4b 所示, 位于 855.8 eV 和 873.6 eV

处的峰分别属于  $\text{Ni}^{2+}$  2p<sub>3/2</sub> 和  $\text{Ni}^{2+}$  2p<sub>1/2</sub>, 结合能为 861.9 和 879.9 eV 附近的峰为 Ni 的卫星峰 (标记为

“Sat.”), 这表明 Ni 以  $\text{Ni}^{2+}$  的状态存在<sup>[20]</sup>。如图 4c 所示, 235.3 和 232.1 eV 处的峰值分别对应于 Mo 3d<sub>3/2</sub>

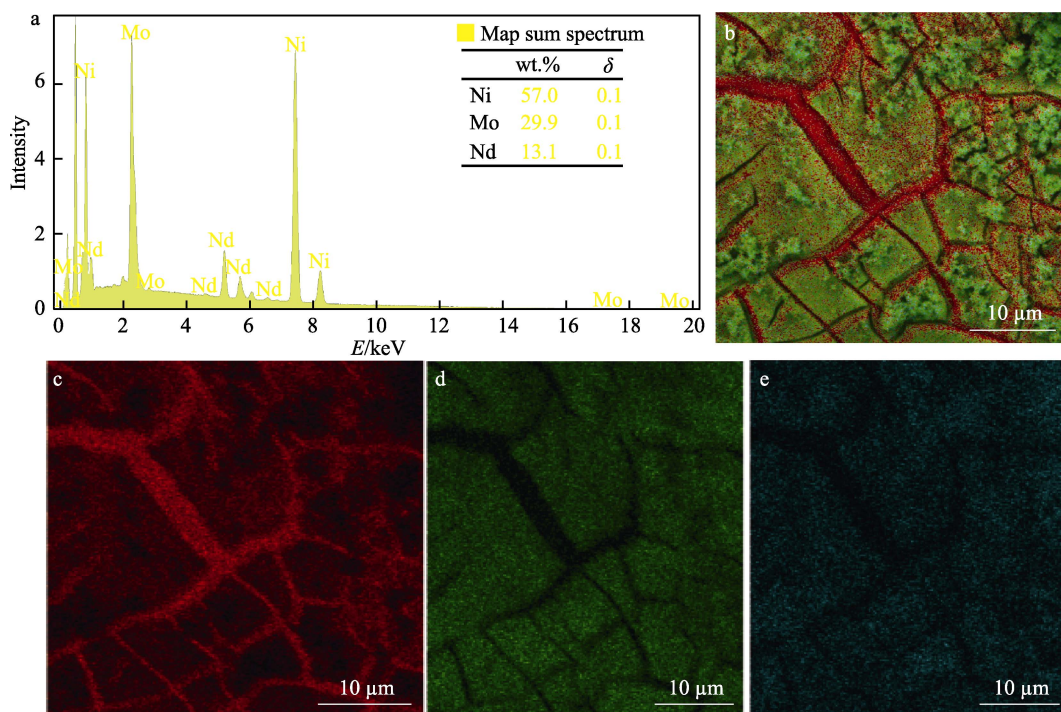


图 2 Ni-Mo-Nd/NF 电极的 EDS 谱图(a); Ni-Mo-Nd/NF EDS Mapping 图(b~c)  
Fig.2 EDS image of Ni-Mo-Nd/NF (a) and EDS Mapping images of Ni-Mo-Nd/NF (b-c)

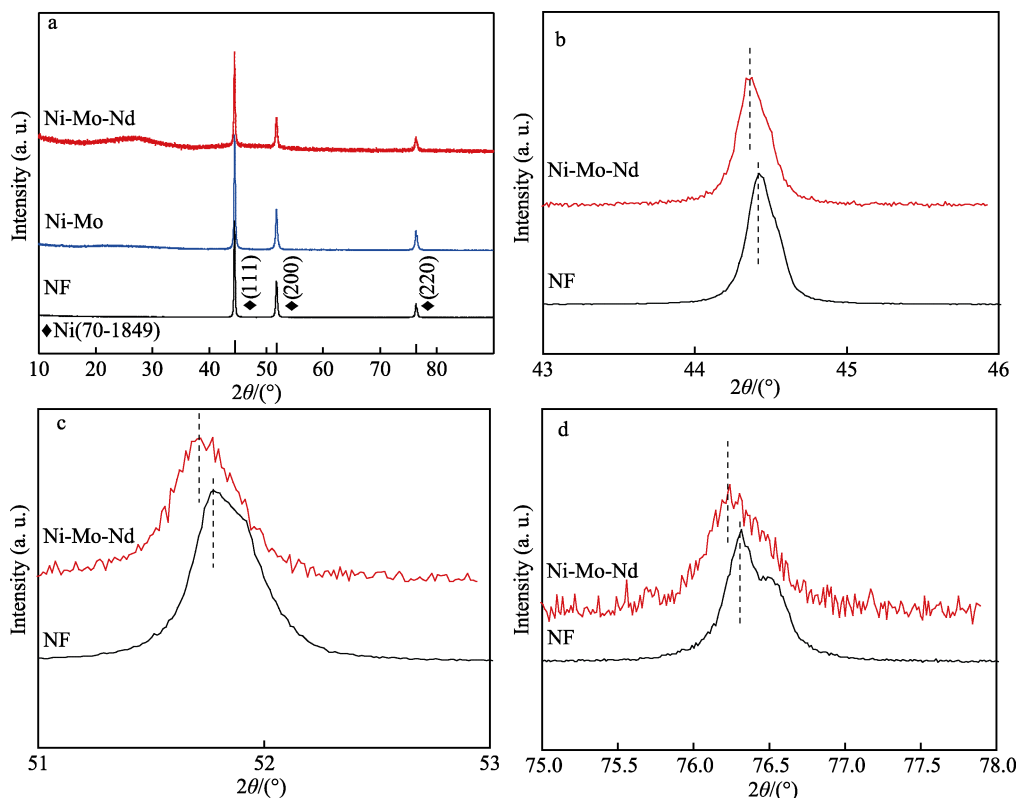


图 3 NF、Ni-Mo/NF 及 Ni-Mo-Nd/NF 电极的 XRD 图谱(a); Ni-Mo-Nd/NF 电极的(111)、(200)及(220)峰相对于 NF 电极的负位移(b~d)  
Fig.3 XRD patterns of Ni foam, Ni-Mo/NF and Ni-Mo-Nd/NF electrodes (a) and the negative shift of the (111), (200) and (220) peaks of Ni-Mo-Nd electrode relative to the NF electrode (b-d)

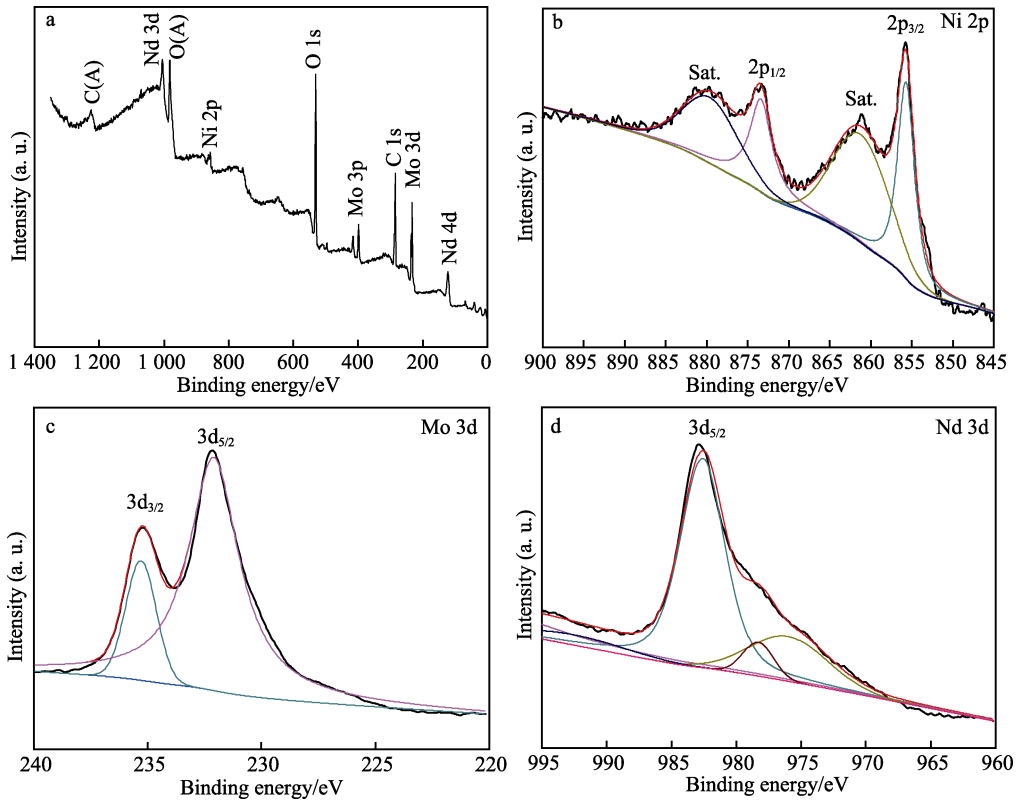


图4 Ni-Mo-Nd/NF电极的XPS图  
Fig.4 XPS spectra of Ni-Mo-Nd/NF electrocatalyst

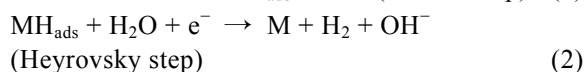
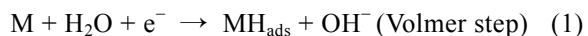
和Mo 3d<sub>5/2</sub>自旋轨道峰<sup>[21]</sup>,表明Mo元素以Mo<sup>6+</sup>状态存在,是电极表面部分Mo发生氧化反应的产物<sup>[21]</sup>。Ni和Mo的氧化态表明电极表面被部分氧化,形成表面钝化膜<sup>[22]</sup>。如图4d所示,982.6 eV处的峰值对应于Nd 3d<sub>5/2</sub>,表明Nd以三价的钕离子存在<sup>[23]</sup>。而XRD测试结果Ni晶格常数变大,这是由于Nd<sup>3+</sup>进入晶格中占据Ni的位置,导致晶格发生畸变。

## 2.2 电化学性能分析

在1 mol/L KOH溶液中,25 °C条件下,以2 mV/s的扫描速率,测量Ni-Mo-Nd/NF及Ni-Mo/NF析氢极化曲线,并以20% (质量分数) Pt/C电极和NF电极进行对比,如图5a所示,Pt/C电极表现出最佳的电催化性能,过电位很小。Ni-Mo-Nd/NF电极在电流密度10 mA/cm<sup>2</sup>时,析氢过电位仅为73 mV,相比Ni-Mo电极( $\eta_{10}=135$  mV, 25 °C),Ni-Mo-Nd/NF电极表现出更好的电催化活性。

根据LSV曲线(图5a)计算了HER动力学的Tafel斜率(图5b)。根据Tafel方程<sup>[24]</sup>:  $\eta=a+b\ln J$ ,当阴极极化, $a=-(RT/(anF))\cdot\ln J_0$ ,  $b=RT/(anF)$ ,其中 $\eta$ 是过电压( $\eta=E_e-E$ ), $J$ 是电流密度, $T$ 是热力学温度, $R$ 是气体常数, $n$ 是转移电子的数量, $F$ 是法拉第常数(96 485 C/mol), $a$ 是传递系数。通过对Tafel曲线的线性拟合,可以得到表观交换电流密度 $J_0$ 。如图5b所示,20% (质量分数) Pt/C、Ni-Mo/NF、

Ni-Mo-Nd/NF电催化剂和NF的Tafel斜率分别约为89、201、147和202 mV/dec,Ni-Mo-Nd/NF电催化剂相比Ni-Mo/NF在碱性介质中表现出更快的析氢反应速率<sup>[25]</sup>。根据文献<sup>[26]</sup>,在碱性电解质中,根据不同的控制步骤,可以分为以下3种机制。



根据Tafel斜率可以判断电催化剂的析氢机理,Volmer反应、Heyrovsky反应及Tafel反应所对应的塔菲尔斜率分别为118、39和29.5 mV/dec,意味着Ni-Mo-Nd/NF遵循Volmer-Heyrovsky机理,Volmer反应为控制步骤,其在析氢反应中电化学吸附过程起控制作用<sup>[27]</sup>。

为了进一步分析电化学催化活性强弱的原因,采用循环伏安法(CV)在不同扫描速度下对样品进行测试,以扫描速度为纵坐标、电流差为横坐标绘制电化学双层电容曲线,由 $C_{dl}$ 估算电催化活性表面积(ECSA)。如图5d所示,Ni-Mo-Nd/NF电极的 $C_{dl}$ 为4.39 mF/cm<sup>2</sup>,明显高于Ni-Mo(2.73 mF/cm<sup>2</sup>),表明Nd的掺杂可以极大增加电极真实表面积。

催化剂的稳定性是评价析氢材料性能优劣的关键指标。对电极进行循环伏安耐久性测试,结果如图6a所示,2 000圈循环前后的LSV曲线只有微小的变

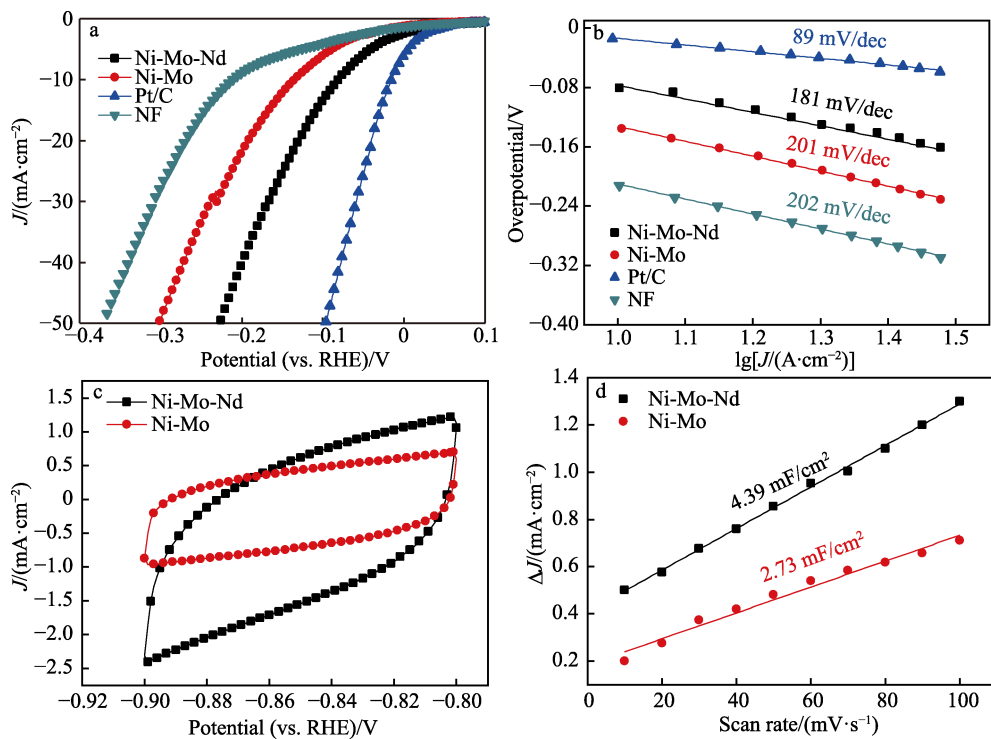


图 5 NF、Pt/C、Ni-Mo/NF 和 Ni-Mo-Nd/NF 电极的 LSV 曲线(a); NF、Pt/C、Ni-Mo/NF 和 Ni-Mo-Nd/NF 电极的 Tafel 曲线(b); Ni-Mo/NF 和 Ni-Mo-Nd/NF 电极在 PBS 溶液中扫描速度 50 mV/s 下的 CV 曲线(c); Ni-Mo/NF 和 Ni-Mo-Nd/NF 电极的扫描速率与电容电流的线性图(d)

Fig.5 IR-Corrected linear sweep voltammetry curves of NF, Pt/C, Ni-Mo/NF and Ni-Mo-Nd/NF (a), Tafel plots of NF, Pt/C, Ni-Mo/NF and Ni-Mo-Nd/NF (b), CVs of Ni-Mo/NF and Ni-Mo-Nd/NF in PBS at scan rate of 50 mV/s (c) and measured capacitive currents plotted as a function of scan rate (d)

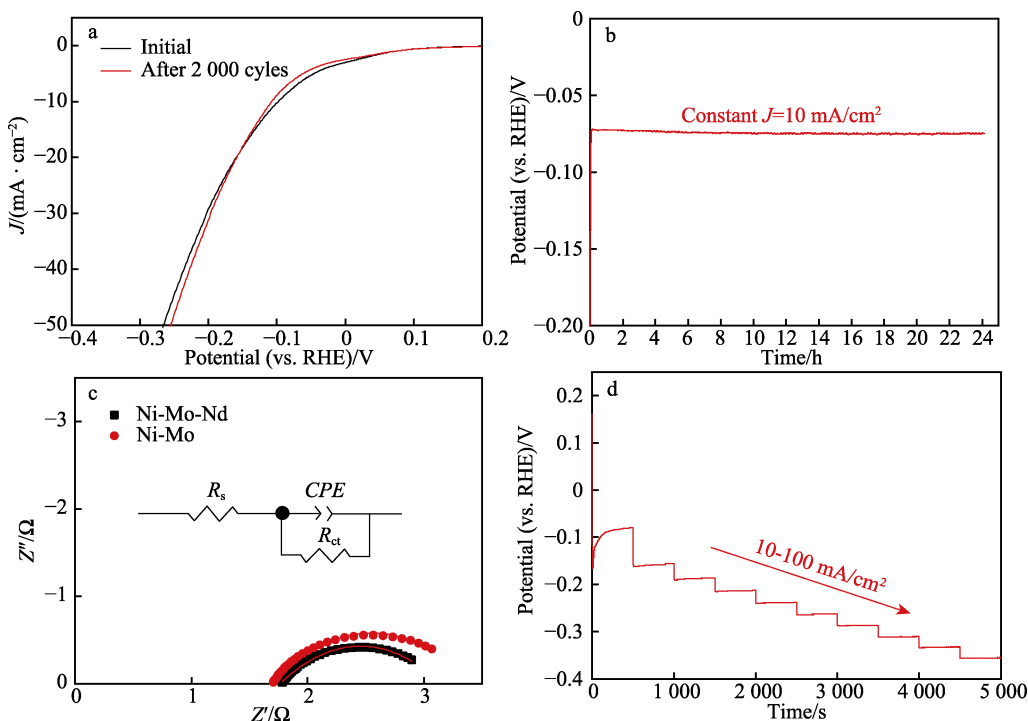


图 6 2000 圈循环伏安扫描前后的 LSV 曲线(a); Ni-Mo-Nd/NF 在 10  $\text{mA}/\text{cm}^2$  电流密度下电解 24 h 的电压-时间曲线(b); Ni-Mo/NF 和 Ni-Mo-Nd/NF 电极的电化学阻抗图谱(插图为等效电路图)(c); Ni-Mo-Nd/NF 在多电流下的稳定性试验(d)

Fig.6 Polarization curves of Ni-Mo-Nd/NF before and after 2000 CV cycles (a), chronopotentiometry curve of Ni-Mo-Nd/NF at constant current density of 10  $\text{mA}/\text{cm}^2$  (b), impedance Nyquist plots of Ni-Mo/NF and Ni-Mo-Nd/NF (c) and stability test of Ni-Mo-Nd/NF carried out at multiple currents (d)

化, 表明 Ni-Mo-Nd/NF 电极在碱性介质中具有良好的电化学稳定性。在恒电流下对 Ni-Mo-Nd/NF 电极电解 24 h, 结果如图 6b 所示, 电极电压保持稳定, 表明电极具有较好的催化稳定性。同时, 利用电化学阻抗法 (EIS) 研究了 Ni-Mo-Nd/NF 和 Ni-Mo 电催化剂的电荷转移速率和电化学动力学。图 6c 为 -200 mV 过电位下的 Nyquist 曲线, 其中的插图为等效电路, 拟合阻抗数据, 包括电解质溶液电阻 ( $R_s$ )、恒相角电容 (CPE) 和电荷转移电阻 ( $R_{ct}$ ), 拟合数据表明与 Ni-Mo/NF 电极 (1.702 Ω) 相比, Ni-Mo-Nd/NF 电极的  $R_{ct}$  值较低 (1.352 Ω), 表明其具有较高的电导率和较低的电荷电阻, 因此其具有良好的电催化性能。为了探究电催化剂在不同电位下的稳定状态, 在 1.0 mol/L KOH 条件下, 从 10 mA/cm<sup>2</sup> 到 100 mA/cm<sup>2</sup>, 测量了 Ni-Mo-Nd/NF 电极的分布电解电位曲线 (图 6d)。在测试中, 每个电流密度持续 500 s。稳定的电位值和良好的电压响应表明 Ni-Mo-Nd/NF 电极具有优良的传质性能。

### 3 结论

本研究通过简单可行的一步恒流电沉积, 在泡沫镍上合成了 Ni-Mo-Nd/NF 电催化剂。制备的 Ni-Mo-Nd/NF 电极在碱性介质中表现出良好的 HER 活性, 电流密度为 10 mA/cm<sup>2</sup>, 过电位为 73 mV。与 Ni-Mo/NF 电催化剂相比, Nd 掺杂后更细的球形纳米颗粒团聚在电极表面, 可以为 HER 提供更多的反应位点, 这与 ECSA 得出的结论一致。Ni-Mo-Nd/NF 电极优异的 HER 性能可归因于其表面形貌、较好的内在活性和稳定性。

### 参考文献:

- [1] PHAM N N T, KANG S G, KIM H J, et al. Catalytic Activity of Ni<sub>3</sub>Mo Surfaces for Hydrogen Evolution Reaction: A Density Functional Theory Approach[J]. *Applied Surface Science*, 2021, 537: 147894.
- [2] JIAO L, LIU E S, HWANG S, et al. Compressive Strain Reduces the Hydrogen Evolution and Oxidation Reaction Activity of Platinum in Alkaline Solution[J]. *ACS Catalysis*, 2021, 11(13): 8165-8173.
- [3] KIM K, TIWARI A P, HYUN G, et al. Continuous 3D-Nanopatterned Ni-Mo Solid Solution as a Free-Standing Electrocatalyst for the Hydrogen Evolution Reaction in Alkaline Medium[J]. *Journal of Materials Chemistry A*, 2021, 9(12): 7767-7773.
- [4] YANG M Y, JIAO L, DONG H L, et al. Conversion of Bimetallic MOF to Ru-Doped Cu Electrocatalysts for Efficient Hydrogen Evolution in Alkaline Media[J]. *Science Bulletin*, 2021, 66(3): 257-264.
- [5] CHEN L L, LASIA A. Hydrogen Evolution Reaction on Nickel-Molybdenum Powder Electrodes[J]. *Journal of the Electrochemical Society*, 1992, 139(12): 3458-3464.
- [6] RODRÍGUEZ-VALDEZ L M, ESTRADA-GUEL I, ALMERAYA-CALDERÓN F, et al. Electrochemical Performance of Hydrogen Evolution Reaction of Ni-Mo Electrodes Obtained by Mechanical Alloying[J]. *International Journal of Hydrogen Energy*, 2004, 29(11): 1141-1145.
- [7] GENNERO DE CHIALVO M R, CHIALVO A C. Hydrogen Evolution Reaction on Smooth Ni(1-x)+Mo(x) Alloys (0 ≤ x ≤ 0.25)[J]. *Journal of Electroanalytical Chemistry*, 1998, 448(1): 87-93.
- [8] LIU W, TAN W Y, HE H W, et al. One-Step Electrodeposition of Ni-Ce-Pr-Ho/NF as an Efficient Electrocatalyst for Hydrogen Evolution Reaction in Alkaline Medium[J]. *Energy*, 2022, 250: 123831.
- [9] ZHU Y N, CHEN B Q, CHENG T S, et al. Deposit Amorphous Ni-Co-B-RE (RE=Ce,Gd and Nd) on Nickel Foam as a High Performance and Durable Electrode for Hydrogen Evolution Reaction[J]. *Journal of Electroanalytical Chemistry*, 2020, 878: 114552.
- [10] WANG Z R, GAO Q B, LV P, et al. Facile Fabrication of Core-Shell Ni<sub>3</sub>Se<sub>2</sub>/Ni Nanofoams Composites for Lithium Ion Battery Anodes[J]. *Journal of Materials Science & Technology*, 2020, 38: 119-124.
- [11] WU Y H, ZHANG Y, WANG Y X, et al. Potentiostatic Electrodeposited of Ni-Fe-Sn on Ni Foam Served as an Excellent Electrocatalyst for Hydrogen Evolution Reaction[J]. *International Journal of Hydrogen Energy*, 2021, 46(53): 26930-26939.
- [12] HUA W, SUN H H, LIU H Y, et al. Interface Engineered NiMoN/Ni<sub>3</sub>N Heterostructures for Enhanced Alkaline Hydrogen Evolution Reaction[J]. *Applied Surface Science*, 2021, 540: 148407.
- [13] ANANTHARAJ S, SUGIME H, NODA S. Surface Amorphized Nickel Hydroxy Sulphide for Efficient Hydrogen Evolution Reaction in Alkaline Medium[J]. *Chemical Engineering Journal*, 2021, 408: 127275.
- [14] GAO Y, HE H W, TAN W Y, et al. One-Step Potentiostatic Electrodeposition of Ni-Se-Mo Film on Ni Foam for Alkaline Hydrogen Evolution Reaction[J]. *International Journal of Hydrogen Energy*, 2020, 45(11): 6015-6023.
- [15] ZHANG P, TAN W Y, HE H W, et al. Binder-Free Quaternary Ni-Fe-W-Mo Alloy as a Highly Efficient Electrocatalyst for Oxygen Evolution Reaction[J]. *Journal of Alloys and Compounds*, 2021, 853: 157265.
- [16] LIU W, TAN W Y, HE H W, et al. Electrodeposition of Self-Supported Ni-Mg-La Electrocatalyst on Ni Foam for Efficient Hydrogen Evolution Reaction[J]. *Electrochimica Acta*, 2022, 411: 140058.
- [17] WU L, GUO X H, XU Y, et al. Electrocatalytic Activity of Porous Ni-Fe-Mo-C-LaNi<sub>5</sub> Sintered Electrodes for Hydrogen Evolution Reaction in Alkaline Solution[J]. *RSC Advances*, 2017, 7(51): 32264-32274.

- [18] BALAJI D, ARUNACHALAM P, DURAIMURUGAN K, et al. Highly Efficient  $\text{Ni}_{0.5}\text{Fe}_{0.5}\text{Se}_2/\text{MWCNT}$  Electrocatalyst for Hydrogen Evolution Reaction in Acid Media[J]. International Journal of Hydrogen Energy, 2020, 45(13): 7838-7847.
- [19] JIN X, LI J, CUI Y T, et al. In-Situ Synthesis of Porous  $\text{Ni}_2\text{P}$  Nanosheets for Efficient and Stable Hydrogen Evolution Reaction[J]. International Journal of Hydrogen Energy, 2019, 44(12): 5739-5747.
- [20] WANG X D, HU Q, LI G D, et al. Regulation of the Adsorption Sites of  $\text{Ni}_2\text{P}$  by Ru and S Co-Doping for Ultra-Efficient Alkaline Hydrogen Evolution[J]. Journal of Materials Chemistry A, 2021, 9(28): 15648-15653.
- [21] CHEN J, TANG Y M, WANG S H, et al. Ingeniously Designed Ni-Mo-S/ $\text{ZnIn}_2\text{S}_4$  Composite for Multi-Photocatalytic Reaction Systems[J]. Chinese Chemical Letters, 2022, 33(3): 1468-1474.
- [22] MA P Y, ZHAO M M, ZHANG L, et al. Self-Supported High-Entropy Alloy Electrocatalyst for Highly Efficient  $\text{H}_2$  Evolution in Acid Condition[J]. Journal of Materials, 2020, 6(4): 736-742.
- [23] ILANCHEZHIYAN P, MOHAN KUMAR G, SIVA C, et al. Aid of Cobalt Ions in Boosting the Electrocatalytic Oxygen and Hydrogen Evolution Functions of  $\text{NdFeO}_3$  Perovskite Nanostructures[J]. Journal of Materials Research and Technology, 2021, 11: 2246-2254.
- [24] AMAYA Á A, GONZÁLEZ C A, NIÑO-GÓMEZ M E, et al. XPS Fitting Model Proposed to the Study of Ni and La in Deactivated FCC Catalysts[J]. Journal of Electron Spectroscopy and Related Phenomena, 2019, 233: 5-10.
- [25] ZÄHR J, OSWALD S, TÜRPE M, et al. Characterisation of Oxide and Hydroxide Layers on Technical Aluminum Materials Using XPS[J]. Vacuum, 2012, 86(9): 1216-1219.
- [26] WEI Y, ZHANG X, ZHAO Z L, et al. Controllable Synthesis of P-Doped  $\text{MoS}_2$  Nanopetals Decorated N-Doped Hollow Carbon Spheres towards Enhanced Hydrogen Evolution[J]. Electrochimica Acta, 2019, 297: 553-563.
- [27] CHEN Z G, GONG W B, CONG S, et al. Eutectoid-Structured WC/W<sub>2</sub>C Heterostructures: A New Platform for Long-Term Alkaline Hydrogen Evolution Reaction at Low Overpotentials[J]. Nano Energy, 2020, 68: 104335.

(上接第 182 页)

- [20] CHATTOPADHYAY D K, WEBSTER D C. Hybrid Coatings from Novel Silane-Modified Glycidyl Carbamate Resins and Amine Crosslinkers[J]. Progress in Organic Coatings, 2009, 66(1): 73-85.
- [21] SULEIMAN R, ESTAITIE M, MIZANURAHMAN M. Hybrid Organosiloxane Coatings Containing Epoxide Precursors for Protecting Mild Steel Against Corrosion in a Saline Medium[J]. Journal of Applied Polymer Science, 2016, 133(38): e43947.
- [22] SULEIMAN R, DAFALLA H, EL ALI B. Novel Hybrid Epoxy Silicone Materials as Efficient Anticorrosive Coatings for Mild Steel[J]. RSC Advances, 2015, 5(49): 39155-39167.
- [23] ESFANDEH M, MIRABEDINI S M, PAZOKIFARD S, et al. Study of Silicone Coating Adhesion to an Epoxy Undercoat Using Silane Compounds[J]. Colloids and Surfaces A: Physicochemical and Engineering Aspects, 2007, 302(1/2/3): 11-16.
- [24] RATH S K, CHAVAN J G, SASANE S, et al. Coatings of PDMS-Modified Epoxy via Urethane Linkage: Segmental Correlation Length, Phase Morphology, Thermomechanical and Surface Behavior[J]. Progress in Organic Coatings, 2009, 65(3): 366-374.
- [25] HENG Z G, ZENG Z, CHEN Y, et al. Silicone Modified Epoxy Resins with Good Toughness, Damping Properties and High Thermal Residual Weight[J]. Journal of Polymer Research, 2015, 22(11): 203.
- [26] XUE J J, WANG L, FAN Y, et al. Mechanically Enhanced Self-Stratified Acrylic/Silicone Antifouling Coatings[J]. Coatings, 2022, 12(2): 232.